Journal of Translational Medicine

RESEARCH

Open Access

Advancing precision medicine in esophageal squamous cell carcinoma using patient-derived organoids

Suya Shen[1], Bing Liu[2], Wenyan Guan[3], Ziyao Liu[4], Yuqing Han[1], Yingzhe Hu[5], Yiqiang Chen[4], Siyuan Liu[4], Jian He[6], Zhiwen Li[3], Weifeng Tang[7], Pengju Zhang[8], Wei Ren[9*], Yudong Qiu[1*], Hongping Zheng[8,10*] and Jingjing Li[4*]

Abstract

Background Patient-derived organoids (PDOs) represent a promising approach for replicating the characteristics of original tumors and facilitating drug testing for personalized treatments across diverse cancer types. However, clinical evidence regarding their application to esophageal cancer remains limited. This study aims to evaluate the efficacy of implementing PDOs in clinical practice to benefit patients with esophageal squamous cell carcinoma (ESCC).

Methods Fresh surgical biopsies were obtained from patients with esophageal cancer for the establishment of PDOs. These PDOs were subsequently characterized through histological analysis. A customized drug panel, based on standard-of-care chemotherapy regimens, was applied to the PDOs. The resulting drug sensitivity profiles were then correlated with the clinical responses observed in individual patients undergoing actual treatment.

Results A total of 34 PDOs were successfully established with a 61.8% success rate. The classification method based on chemotherapy sensitivity closely corresponded to clinical responses. The paclitaxel plus cisplatin (TP)-sensitive group demonstrated significantly longer progression-free survival (PFS) compared to the resistant groups, Hazard ratio (HR), 5.12; 95% confidence intervals (CI 0.58–44.71; $p < 0.05$), thus illustrating the potential of this approach for guiding personalized treatment strategies.

Conclusion Organoid biobanks were established across multiple institutes to facilitate PDOs-based functional precision medicine. The findings demonstrate that this framework offers robust predictive value in clinical settings, enhances precision therapeutics, and advances drug discovery for esophageal cancer.

Keywords Esophageal squamous cell carcinoma, Organoids, Chemotherapy, Precision medicine

*Correspondence:
Wei Ren
renwei@njglyy.com
Yudong Qiu
yudongqiu510@nju.edu.cn
Hongping Zheng
80885626@qq.com
Jingjing Li
jijilee_82@163.com
Full list of author information is available at the end of the article

Graphical Abstract

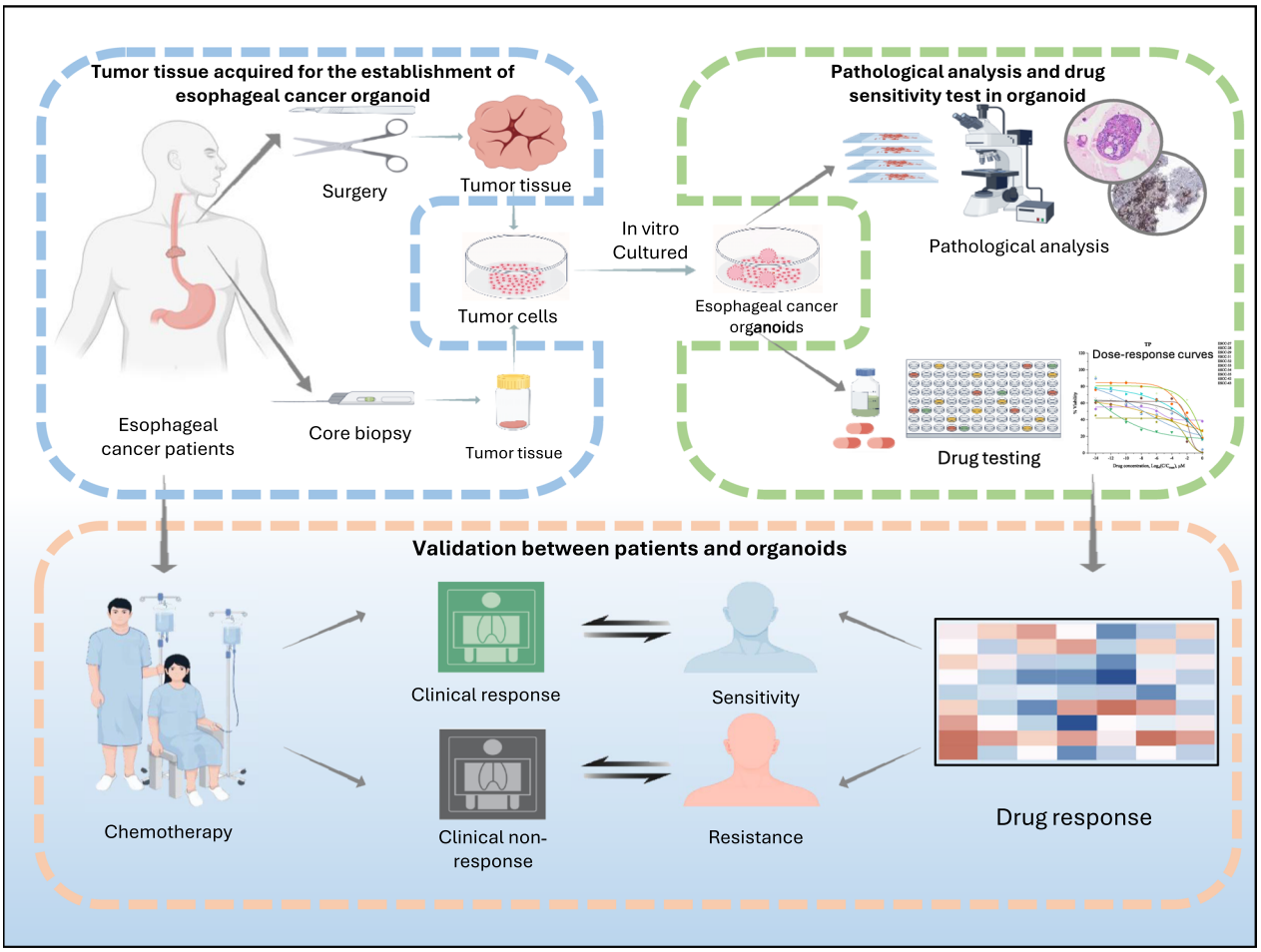

Introduction

Esophageal carcinoma (EC) poses a significant threat to public health due to its increasing incidence and inconspicuous symptoms, which often result in late diagnosis and poor prognosis [1]. The conventional standard-of-care treatment forEC involves surgical resection combined with chemotherapy [2–4]. However, nearly 60% of patients fail to benefit from these treatments due to tumor heterogeneity, therapeutic resistance, and substantial side effects [5–7]. Moreover, the growing number of available chemotherapy drugs has made it increasingly challenging for clinicians to select optimal regimens based solely on clinical expertise and patient values. Esophageal adenocarcinoma (EAC) and esophageal squamous cell carcinoma (ESCC) are the two primary pathological types of EC [8]. In the past decade, targeted therapies for advanced stages of esophageal adenocarcinoma (EAC) have been limited and offer minimal benefits, while progress in ESCC has been virtually non-existent [9]. Consequently, current precision medicine strategies for EC remain inadequate, underscoring the need for improved preclinical models to contribute to effective treatments and facilitate personalized therapy.

Numerous studies have focused on identifying significant biomarkers for predicting clinical prognosis, however, reliable preclinical models for evaluating patient responses to chemotherapeutic and targeted agents are lacking [6, 10, 11]. Recently, patient-derived organoids (PDOs) have emerged as a promising tool in precision medicine, with significant potential for modeling patient-specific responses to treatments. Unlike two-dimensional cell lines that grow as flat monolayers, PDOs are cultured in a three-dimensional structure, more accurately

simulating the self-organization and cellular interactions of the tumor microenvironment [12, 13]. Moreover, in contrast to the extended tumorigenic processes required for genetically engineered mouse models and patient-derived xenografts (PDXs), organoids can be generated directly from primary tissue within a reasonable timeframe [14]. PDOs also recapitulate the genetic and morphological characteristics of the parental tumors with a high success rate and enable long-term expansion [15–17]. These advantages have been demonstrated in various primary tumors, including liver [18], pancreas [19], breast [20], colorectal cancer [21], and other solid tumors. The fidelity of PDOs makes them highly valuable for predicting patient-specific therapy responses and personalizing treatment strategies. However, research on esophageal cancer organoids, particularly esophageal squamous cell carcinoma organoids (ESCOs), remains limited, with scarce clinical evidence and a lack of comprehensive studies on their tissue characteristics. The advancement of esophageal organoids provides significant molecular and mechanistic insights into diverse physiological and pathological dynamics, driving progress in furthering translational research and personalized medicine [22, 23]. A recent study by Li et al. developed a panel of EAC organoids that accurately recapitulate the characteristics of primary tumors, including their morphology, genomic profiles, and transcriptomic landscape, this study demonstrated the feasibility of moderate throughput drug screening to identify new therapeutic targets, indicating that EAC organoids serve as a powerful tool for studying clonal evolution and offer a valuable preclinical platform for developing precision therapeutics. PDOs are valuable for evaluating treatment effectiveness in a preclinical setting [14]. In ESCC, Kijima's laboratory successfully established and characterized PDOs, emphasizing their utility in investigating tumor heterogeneity, generating drug-response assays, and uncovering mechanisms of drug resistance [22, 24]. Advancements in ESCOs hold significant promises for overcoming treatment challenges in esophageal cancer, paving the way for more effective precision medicine strategies to combat this deadly disease. However, further research is necessary to conduct comprehensive profiling and assess the application of in-vitro drug testing in ESCC. To bridge these gaps,, we established a robust protocol for generating primary ESCOs culture from multiple centers, developed a standardized drug testing platform utilizing organoids, and initiated a retrospective clinical study to evaluate the potential of PDOs as predictive biomarkers for chemotherapeutic sensitivity in ESCC patients. Our case studies demonstrated that the drug responses observed in PDOs closely align with the clinical response of patients, highlighting the significant potential of this approach to advance precision medicine in esophageal cancer.

Materials and methods

Participant selection and study design

Adults (age ≥ 18 years) with histologically and radiologically confirmed esophageal cancer were enrolled in the study based on clinical and radiologic evidence. The primary objective was to establish efficient culture methods for PDOs suitable for drug testing and to evaluate their potential in correlating patient outcomes with standard-of-care treatments for translational research. Figure 1 illustrates the study design flowchart. Esophageal cancer specimens were primarily obtained from patients undergoing surgical resection or endoscopic biopsy at Nanjing Drum Tower Hospital, Beijing Cancer Hospital, and Jiangsu Hospital of Traditional Chinese Medicine. The Institutional Ethics Committees approved all tissue donations and experiments (Approval number: 2021-237-02). Two independent pathologists confirmed the histological characteristics of the samples. Following surgical tumor resection, patients received clinically verified standard-of-care chemotherapy regimens based on physician's empirical choice. Comprehensive clinical characteristics were obtained and recorded using data collection forms from the hospitals' internal electronic medical records system. Clinical responses were assessed using RECIST 1.1 criteria [25]. In some instances, comprehensive clinical data were unavailable due to loss of follow-up or patients' unwillingness to accept the suggested adjuvant therapy. Participant enrollment occurred from September 2021 to August 2022.

Patient material processing and generation of organoids

Patient specimens were washed with Hanks' Balanced Salt Solution (HBSS, Sigma) and minced into 1–2 mm^3 pieces using sterile scissors. The tissue underwent enzymatic digestion at 37 °C for 30 min with 1 mg/mL collagenase type II (Worthington), 1 mg/mL collagenase type IV (Worthington), 0.1 mg/mL DNase I (Worthington), and 100 U/mL penicillin–streptomycin (Life Technologies). The resulting fragments suspension was filtered through a 70-μm strainer, and undigested fragments were subjected to an additional 20 min of digestion before being re-filtered. The isolated cell suspension was resuspended in 70% ice-cold Matrigel (354,234, Corning). After 10 min, the solidified Matrigel were then supplemented with ESCOs culturing media: Advanced DMEM/F12 (Gibco) was supplemented with 10 mM HEPES (Gibco), 1 × GlutaMAX (Gibco), 100 U/mL penicillin–streptomycin (Gibco), 1 × B27 (Gibco), 1 × N2 (Gibco), 50 ng/mL EGF (Novoprotein), 10 ng/mL FGF-10 (Novoprotein), 100 ng/mL Noggin (Novoprotein),

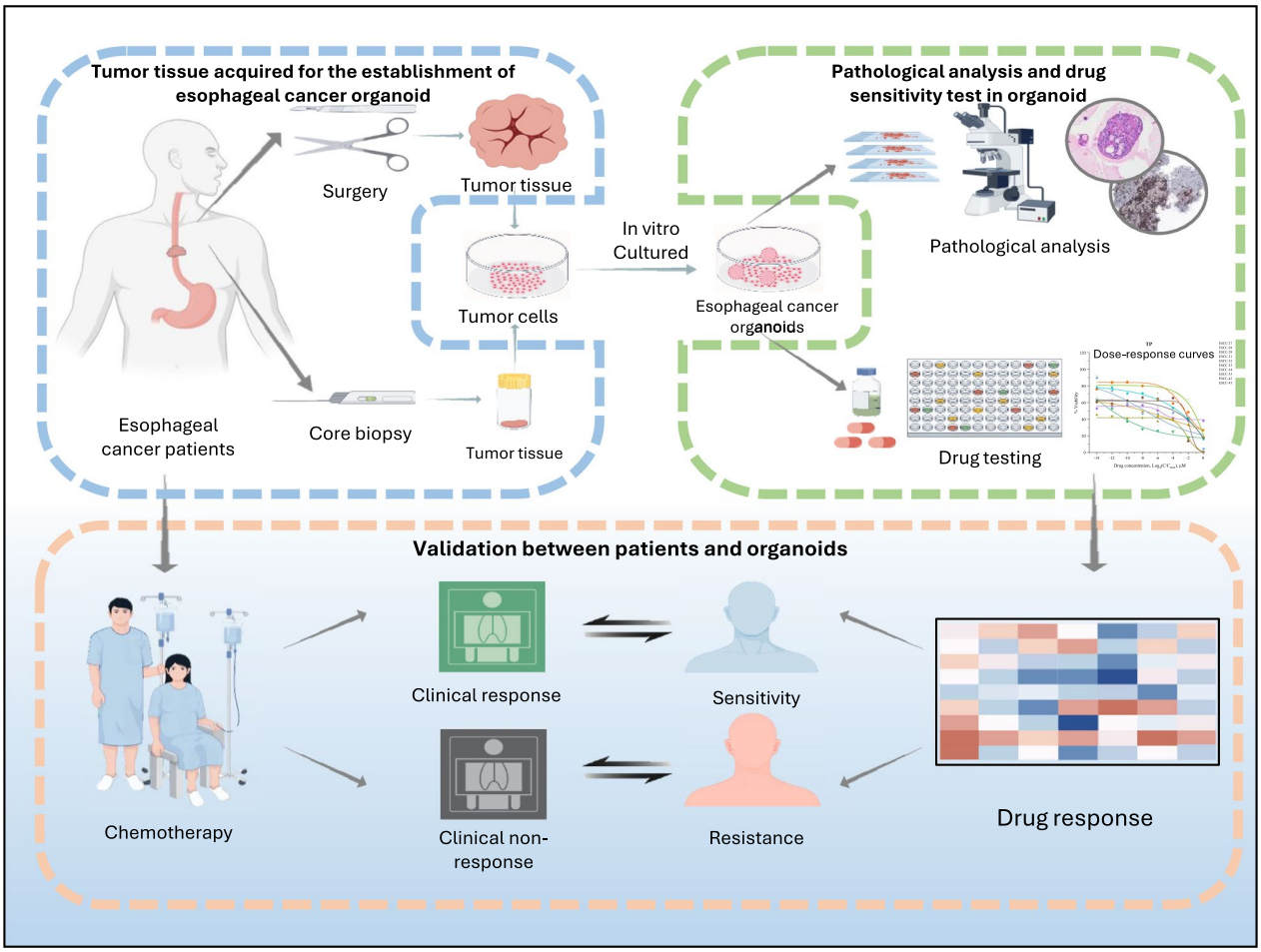

Fig. 1 Graphical abstract of study design. Fresh ESCC specimens were obtained from patients and processed following the outlined methodology. Standard-of-care drug testing was conducted on PDOs, and the results were analyzed in correlation with the clinical responses observed in individual patients

250 nM A83-01 (Beyotime), 10 μM SB202190 (Beyotime), 100 ng/mL Wnt3a (Novoprotein), 100 ng/mL R-spondin 1 (Novoprotein), 1 mM N-Acetylcysteine (Sigma), and 10 μM Y-27632 (Beyotime). Organoids were incubated at 37 °C in 5% CO_2, with the medium changed every 2–3 days. For passaging, organoids were split every 1–2 weeks at a ratio of 1:2 or 1:3. Organoids were collected and digested with TrypLE Express (Gibco) at 37 °C for 5–10 min, then washed with Advanced DMEM/F12 and resuspended in Matrigel, supplemented with organoid culture medium. Organoid quantification was conducted using bright-field imaging with an IX73 microscope (Olympus, Tokyo, Japan).

Histology and immunohistochemistry

Surgical resection tissues were fixed in 10% formalin overnight and embedded in paraffin blocks after dehydration. Confluent organoids were collected, rinsed with ice-cold PBS to dissolve the Matrigel, and fixed in 10% formalin for 1 h. The organoids were then settled by gravity and embedded in paraffin. All sample blocks were sectioned into 3-μm-thick slides, followed by dewaxing, rehydration, and standard hematoxylin and eosin (H&E) staining. For immunohistochemistry (IHC) staining, paraffin slides underwent deparaffinization and rehydration, then were incubated with primary antibodies specific to p53 (1:100, clone D-O7, ZSGB-Bio, ZM-0408), CK5/6 (1:100, clone OTI1C7, ZSGB-Bio, ZM-0313), SOX-2 (1:100, EP103, ZSGB-Bio, ZA-0571), and KLF5 (1:200, Invitrogen, PA5-27,876) at 4 °C overnight. Subsequently, sections were washed and incubated with secondary antibody at room temperature for 1 h, with negative controls applied to all samples. The slides were scanned and imaged using a microscope (Nikon, Eclipse CI, Japan). The immunoreactivity of the slides was assessed independently by two senior pathologists who were blinded to this study.

QuPath software was utilized for digital pathology and image analysis.

Drug screening assays

Drug testing was conducted with modifications to accommodate the 384-well format, as previously validated [26]. The primary organoids in good condition were collected and dissociated into single cells by incubating in TrypLE (Gibco) for 10 min. The single cells resuspended in the organoid culture medium with 5% Matrigel, and approximately 2000 cells were seeded per well of 384-well plates (Thermo Fisher Scientific, 242,764). They were cultured for 3 days to allow cell recovery before drug treatment. Eight concentration points with fourfold dilutions were set for each single drug or drug combination and dispensed using liquid-handling robots, with each concentration tested in triplicate. The starting concentrations for the monotherapy treatments were 100 μM for cisplatin (DDP), 100 μM for5-fluorouracil (5-FU), 5 μM for paclitaxel, and 5 μM for vinorelbine. For combination therapy, paclitaxel and cisplatin (TP) treatments, vinorelbine and cisplatin (NP) treatments, and 5-fluorouracil plus cisplatin (FP) treatments were assayed in triplicate drug matrices. The starting concentrations were the same as those used in the monotherapy treatments. Similarly, for FOLFIRINOX (FFX) treatment, each component began at a concentration of 100 μM. DMSO at 0.5% (v/v) served as the negative (vehicle) control. Cell viability was assayed using Cell Counting-Lite 3D Luminescent Cell Viability Assay (Vazyme) following 5 days of drug treatment. Luminescent detection of cell viability was performed after 25 min of incubation with the cells at room temperature. In-vitro responses were evaluated using dose–response curves for single agents and drug combinations. IC50 and AUC (area under the curve) values were determined using Origin 2022 and GraphPad Prism 8.0. Normalized AUC values were calculated by dividing the AUC of each compound by the maximum AUC observed within the measured concentration range.

Quantification and statistical analysis

Statistical analyses for each dataset are detailed in the corresponding figure legends. Clinical data were extracted and managed from individual electronic health records. Group comparisons were conducted using the chi-squared test (or Fisher's exact test when appropriate) for categorical variables and the student's t-test for continuous variables. Tumor response was assessed according to RECIST guidelines (version 1.1) [25]. Data analyses were performed using Origin 2022 (OriginLab Corporation, USA) employing nonlinear regression (curve fit). Progression-free survival (PFS) differences were evaluated using Kaplan–Meier survival curves and the log-rank test with GraphPad Prism 8. p values < 0.05 were considered statistically significant.

Results

Patient demographics and tumor characteristics

This study involved 55 human samples from individual patients with confirmed pathological ESCC diagnoses for PDO generation. Fifty specimens were obtained through surgical resection from Nanjing Drum Tower Hospital and Peking University Cancer Hospital, while five samples were isolated from endoscopy biopsies at Jiangsu Chinese Medicine Hospital (Supplementary Table S1). Figure 2A presents a consort diagram illustrating the sample distribution. Baseline characteristics included patient demographics, tumor location, histological classification, cancer stage, and primary treatment. All samples were derived from primary tumors without distant metastasis at collection time, classified as ESCC, with a median patient age of 64 years. 14 tumors (46.67%) were moderately differentiated, and 27 tumors (90%) were located in the middle or lower esophagus, aligning with EC epidemiology [27]. Four organoids generated from esophagogastroscopy biopsy were associated with patients who were lost to follow-up. Of the 26 patients who underwent surgery, 14 received subsequent adjuvant chemotherapy, including six who underwent neoadjuvant chemotherapy, indicating tissue acquisition in a post-neoadjuvant condition. Among these, one patient developed a low platelet count after two cycles of paclitaxel combined with platinum treatment, preventing the continuation of subsequent regimens. Another patient received S-1 (Taiho Pharmaceutical Co., Ltd), an oral fluoropyrimidine, as adjuvant therapy but was lost to follow-up three months post-surgery [28].

Generation and histological characterization of ESCOs

Fresh ESCC tissue samples were obtained from esophagectomy or esophagogastroscopy biopsy and seeded into an esophageal cancer organoid culturing medium as described in the methods section. The study design is illustrated in Fig. 2B. Organoids were cultivated in a Matrigel-supported growth medium to facilitate expansion. As shown in Fig. 2A, 17 cases failed to initiate a culture due to insufficient tumor cells or lack of expansion beyond passage two, while four organoids experienced bacterial contamination during cultivation. Overall, we achieved a ~ 62% PDO culture success rate (34 of 55 cultures) throughout the study, aligning with previous reports on gastrointestinal cancers [6, 29]. For 4 organoids, the clinical response of the corresponding patients was not evaluable due to a short follow-up

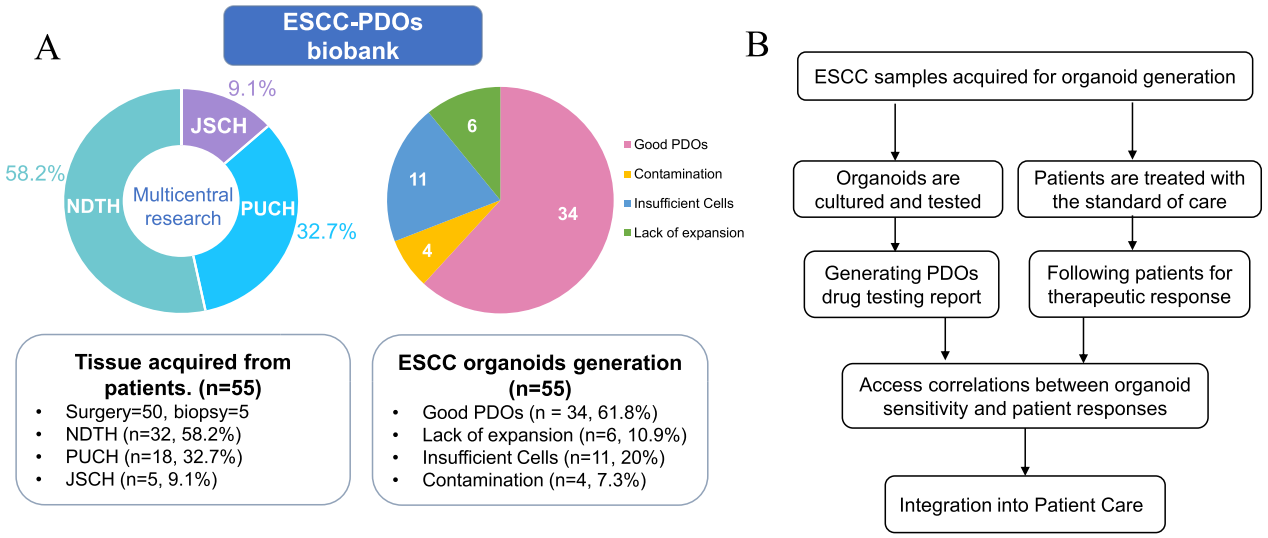

Fig. 2 Characterization and establishment of ESCC organoids. **A** Pie chart illustrating the characteristics of the organoid biobank derived from multicenter patients and the isolation efficiency rate for establishing cultures from surgical resection and biopsy specimens. NDTH, Nanjing Dump Tower Hospital; PUCH,Beijing Cancer Hospital; JSCH, Jiangsu Chinese Medicine Hospital. **B** Flow chart presenting an overview of the study, wherein drug sensitivity based on PDOs was evaluated in comparison with the original patient's chemotherapy response

period. Ultimately, drug testing was conducted on the remaining 30 organoid lines, with the patient's demographic and clinicopathological characteristics respectively detailed in Table 1 and Supplementary Table S2. Among the 30 drug assay reports, 24 organoids were derived from chemotherapy-naïve tumors, while 6 were derived from chemotherapy-treated tumors.

We subsequently evaluated the histological profiles of the primary tissue and corresponding ESCOs to demonstrate their heterogeneous growth states (Fig. 3). Despite their diverse morphologies, the comparison revealed that the ESCOs replicated notable similarities to the matched original tumors in histopathological features. The characteristic solid and compact structures of the organoids are evident in both bright-field and H&E staining, reflecting a cohesive cellular arrangement that mimics key architectural features of stratified squamous epithelium (Fig. 3A) [14, 23]. Immunohistochemical staining of the organoids and their corresponding tumor tissue also revealed comparable expression levels of the ESCC-specific markers. As observed, CK5/6 is predominantly expressed in keratinizing squamous epithelium, as well as glandular epithelial cells, the consistent expression of CK5/6 in ESCOs supports their fidelity to the tissue of origin [30, 31].p53 is a tumor suppressor gene whose mutations lead to uncontrolled tumorigenesis, p53 expression is observed in approximately 50–90% of ESCC patients and serves as a prognostic marker [32]. Regarding p53 status in our study, the ESCOs reflect the tissue prevalence. Notably, in ESCC17, p53 expression was positive in the basal layer of the tissue, but less pronounced in the cancerous region of the tissue, in line with the lower expression observed in organoids derived particularly from tumor tissue. Consistently, the expression of the tumor differentiation marker KLF5 was comparable between the tumor tissue and PDOs. KLF5 is a transcription factor present in proliferating cells of the gastrointestinal tract, including the esophagus, and is implicated in epithelial homeostasis and tumor progression [33, 34]. Similarly, the sex-determining region Y-box 2 (SOX2) is another key marker involved in the initiation and progression of ESCC [35]. SOX2 is a well-known transcription factor active in embryonic and pluripotent stem cells, essential for maintaining squamous cell lineage, and is associated with ESCC carcinogenesis and stemness [35–37]. The expression of SOX2 in our study further substantiates its alignment with the corresponding histopathological specimens. Interestingly, in ESCO55, SOX2 was positive in the tissue but not in the organoids, suggesting that specific characteristics, such as stem cell renewal capacity, may be diminished during the passage process. Despite this, PDOs remain reliable models for recapitulating the primary characteristics of the original tissue. It is important to acknowledge, however, that PDOs may not fully replicate all aspects of the tissue, as certain features can be altered to varying degrees due to passage-induced changes, microenvironmental differences, and technical limitations inherent to the culture system. Additionally, in ESCO52, the specimen consisted of moderately differentiated squamous cell carcinoma cells,

Table 1 The clinicopathological characteristics of 30 ESCC patients

Characteristics	Groups	N0.(%)
	Total Cases	55
	Drug testing performed	30
Sample source		
	Surgery	26 (86.67%)
	Biopsy	4 (13.33%)
Gender		
	Male	28 (93.33%)
	Female	2 (%)
Age of diagnosis		
	Median (Range)	64 (48–78)
Pathologic initial stage		
	I	3 (10%)
	II	10 (33.33%)
	III	13 (43.33%)
	NA	4
Tumor location		
	Upper	3 (3.33%)
	Middle	10 (33.33%)
	Lower	17(56.67%)
Pathological diagnosis		
	ESCC	30 (100%)
Tumor grade		
	Grade 1	4(13.33%)
	Grade 2	14 (46.67%)
	Grade 3	12 (40%)
Post-surgical treatments		
	Chemotherapy	14 (46.67%)
	Surgery alone	16 (53.33%)

displaying overexpression of CK5/6, p53, and KLF5, with low expression of SOX2. The matched organoid similarly exhibited expression of these markers (Fig. 3B). Collectively, these findings strongly confirmed that the organoids faithfully preserved the histological organization and morphological heterogeneity of the original tumors.

Drug assay of conventional chemotherapeutics in ESCOs

To evaluate the applicability of PDO lines in assessing personalized chemotherapeutic responses, therapeutic profiling was conducted on 30 ESCOs using four commonly employed standard-of-care chemotherapeutic agents: single-agent cisplatin (DDP) and combination therapies—paclitaxel plus cisplatin (TP), vinorelbine plus cisplatin (NP), and 5-fluorouracil plus cisplatin (FP). Each group underwent screening for cell viability, with ESCO response quantified and analyzed through dose–response curves and AUC. The AUC values were normalized by dividing each group's value by its maximum, with the detailed normalized AUC data provided in Supplementary Table S3. The ESCOs profiling revealed significant variability in response to both single and combination chemotherapeutic agents among individual patients (Fig. 4A). Violin plots illustrate the distribution of AUC values, highlighting a spectrum of resistance and sensitivity across the samples (Fig. 4B). Using DDP as a representative drug, individual IC50 and 95% CI from dose–response testing demonstrated that ESCOs exhibit distinct chemotherapeutic response profiles to varying doses of cisplatin (Fig. 4C). The in vitro chemosensitivity of ESCOs to DDP and the combination therapies TP, NP, and FP are presented as standardized AUC values (Fig. 4D). The 10 representative ESCOs described in this study are dispersed throughout the whole group, indicating that they represent a range of sensitivity and resistance. Consequently, ESCOs serve as valuable tools for drug response assays, reflecting diverse responses to various conventional chemotherapeutics. Several ESCOs were also treated with FOLFIRINOX (FFX), partially shown in Fig. 5E. To further elucidate the correlation between ESCO sensitivity results and clinical outcomes, the assays were divided into three subgroups based on the AUC values for each chemotherapeutic agent: the ESCOs with their AUC ranked the top 33% were regarded as the least responsive (resistant ESCOs), those with their AUC ranked the lowest 33% as the most responsive (sensitive ESCOs), and those with their AUC ranked the middle 34% AUC as moderately sensitive ESCOs. Among the 30 ESCOs subjected to drug tests, 14 patients received chemotherapy, with detailed AUC values, sensitivities, and corresponding patient responses presented in Table 2**.** These data suggested that most patients (12/14, 85.71%) in this study were treated with TP, drug assays of conventional chemotherapeutics revealed distinct responses in ESCOs. A comparison of PDOs drug responses and patient outcomes would suggest that certain patients might benefit from alternative treatment strategies tailored to the unique sensitivities of their tumor-derived organoids, highlighting the potential of PDOs to guide precision oncology.

ESCOs represent chemotherapy response and clinical prognosis of ESCC patients

To assess the clinical viability of utilizing PDOs platform for ESCC patients, we analyzed retrospective clinical data and compared the pharmacotyping outcomes of ESCOs with the corresponding patients' clinical responses. Among the 30 ESCOs, 14 were from patients who received chemotherapy: 6 were from patients who underwent neoadjuvant chemotherapy, and 8 were from patients who received adjuvant chemotherapy, with follow-up periods ranging from 2.8 to 22.4 months

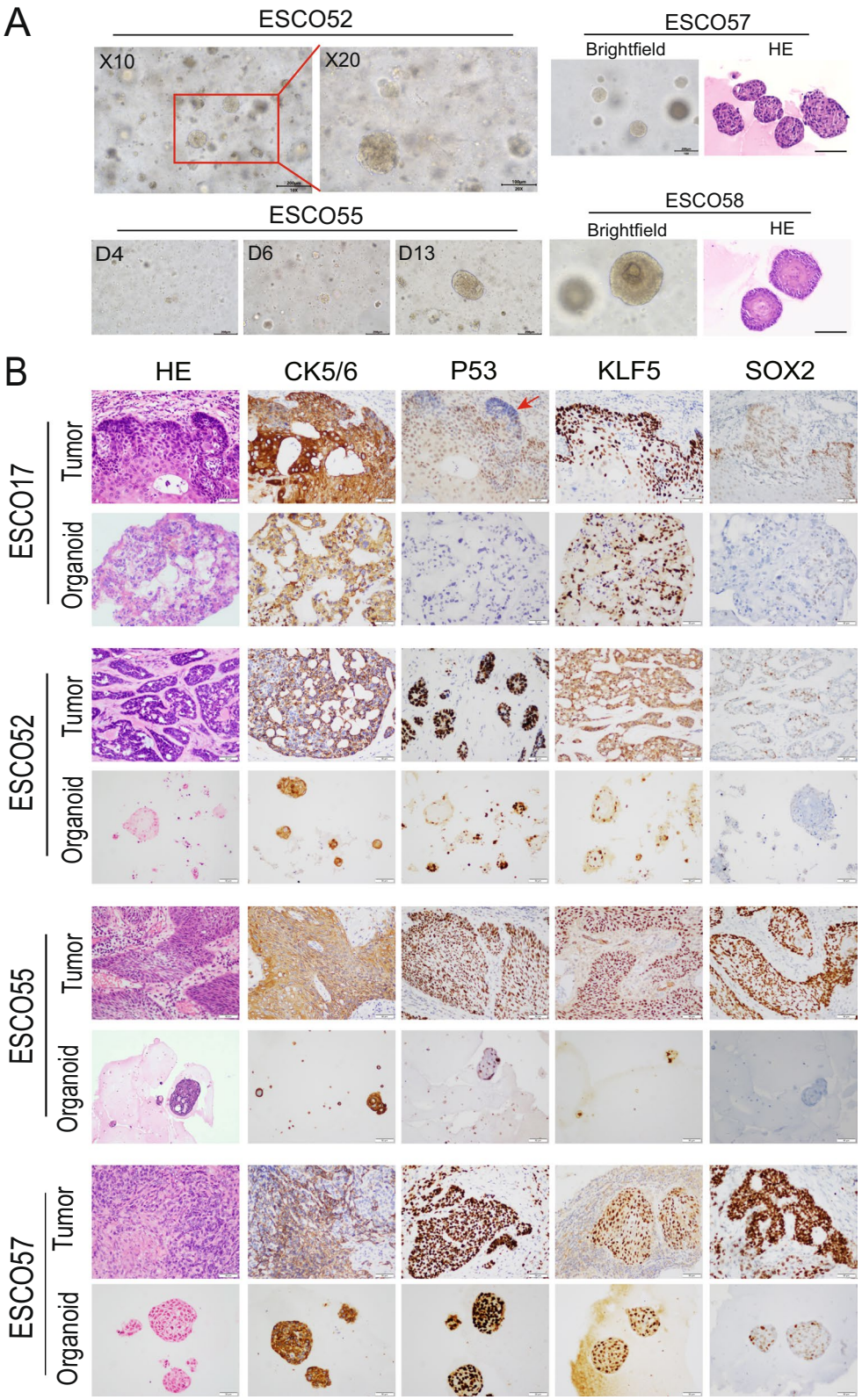

Fig. 3 **A** Bright-field images of ESCO52 at 10 × and 20 × magnification; Time-lapse imaging of ESCO55 growth in 3D Matrigel at Days 4, 6,and 13, respectively. Bright-field images and HE-stained sections of ESCOs forming solid morphology. Scale bar, 200 μm. B. Representative H&E and IHC staining of CK5/6 (Cytokeratin 5/6), P53, KLF5, SOX2 in primary ESCC tissues and organoids. Scale bar, 200 μm

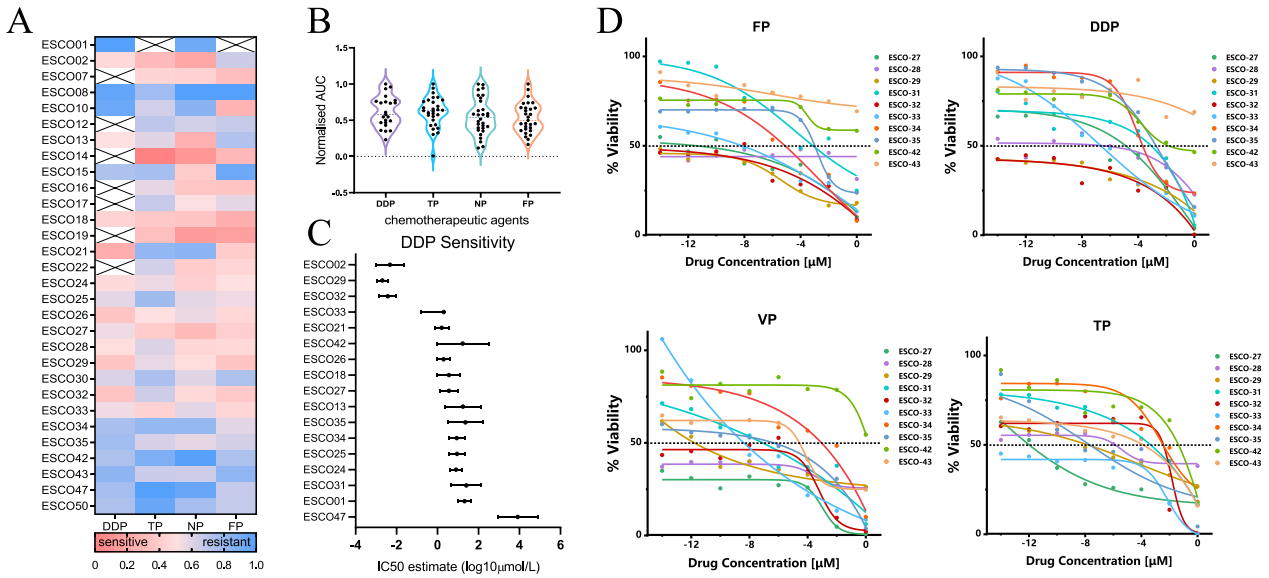

Fig. 4 Drug Assay of Conventional Chemotherapeutics Reveals Distinct Responses in ESCOs. **A** A heatmap illustrates the responses of 30 ESCOs to compounds including cisplatin (DDP), paclitaxel plus cisplatin (TP), vinorelbine plus cisplatin (NP), and 5- fluorouracil plus cisplatin (FP). Normalized AUCs represent chemosensitivity responses, with colors ranging from red (low scores, indicating "sensitive") to blue (high scores, indicating "resistant"). **B** A violin plot presents the normalized AUC values derived from raw dose–response data for the four distinct chemotherapies. **C** The drug profiling distribution for ESCOs (left axis label) demonstrates the IC50 values and 95% CI from dose–response testing with cisplatin (DDP). **D** Drug profiling distribution of 10 representative ESCOs, showing dose–response testing against DDP, TP, NP, and FP, respectively

(Table 2). PFS is defined as the duration from initial treatment until signs of disease progression appear. The treatment responses of ESCC patients classified by clinicians as having a partial response (PR) or stable disease (SD) for more than one year were categorized as indicating a good response (chemotherapy-sensitive). Conversely, patients with progressive disease (PD), including tumor recurrence, metastasis, or disease progression within 1 year were classified as having a poor response (chemotherapy-resistant) as illustrated in Fig. 5A. Despite 2 patients being lost to follow-up, 9 out of the remaining 12 patients who underwent chemotherapy were classified as having a good clinical response, while the other 3 were classified as having a poor response. In the drug assay performed on the ESCOs, the organoids exhibited distinct responses to various chemotherapy regimens (Fig. 5A). As most patients received the TP regimen, we observed that 9 ESCOs demonstrated sensitivity to TP, consistent with their clinical outcomes. However, 2 stage III patients, who were expected to benefit clinically based on their PDO drug assays, exhibited progressive disease, indicating a lack of correlation with the ESCO responses. Lastly, one patient (ESCO25), who experienced rapid disease progression while on paclitaxel plus cisplatin, had an organoid that displayed resistance to TP. In total, 10 out of 12 (83.33%) ESCC patients exhibited consistency in drug response results with those observed in their derived PDOs. Furthermore, we compared the PFS of the two groups of patients based on their sensitivity to the TP regimen. The patients whose ESCOs were sensitive to TP in our assay exhibited significantly higher PFS, suggesting that in vitro sensitivity of ESCOs to TP is associated with a longer clinical response of the corresponding patients. The hazard ratio (HR) was 5.12 (95% CI 0.58–44.71, log-rank test, $P < 0.05$; Fig. 5B). The median timeframe for obtaining drug assay results was approximately 3 weeks, with a range from 2 to 8 weeks, aligning with the typical timeframe for clinical treatment decisions, which are generally made 2 to 3 months after the last treatment to evaluate alternative options. PDO-based drug testing can thus serve as a stratification tool to identify optimal therapeutic combinations for individual patients.

Case report

We closely monitored the disease progression of three patients from whom we derived ESCOs, categorized as sensitive (ESCO10 and ESCO13) or resistant (ESCO25) to their respective treatments. As depicted in Fig. 5C, Patient ESCO10, diagnosed with ESCC, underwent cycles of paclitaxel plus platinum during neoadjuvant chemotherapy, achieving a confirmed PR with a reduction in primary tumor size after 2 months of treatment.

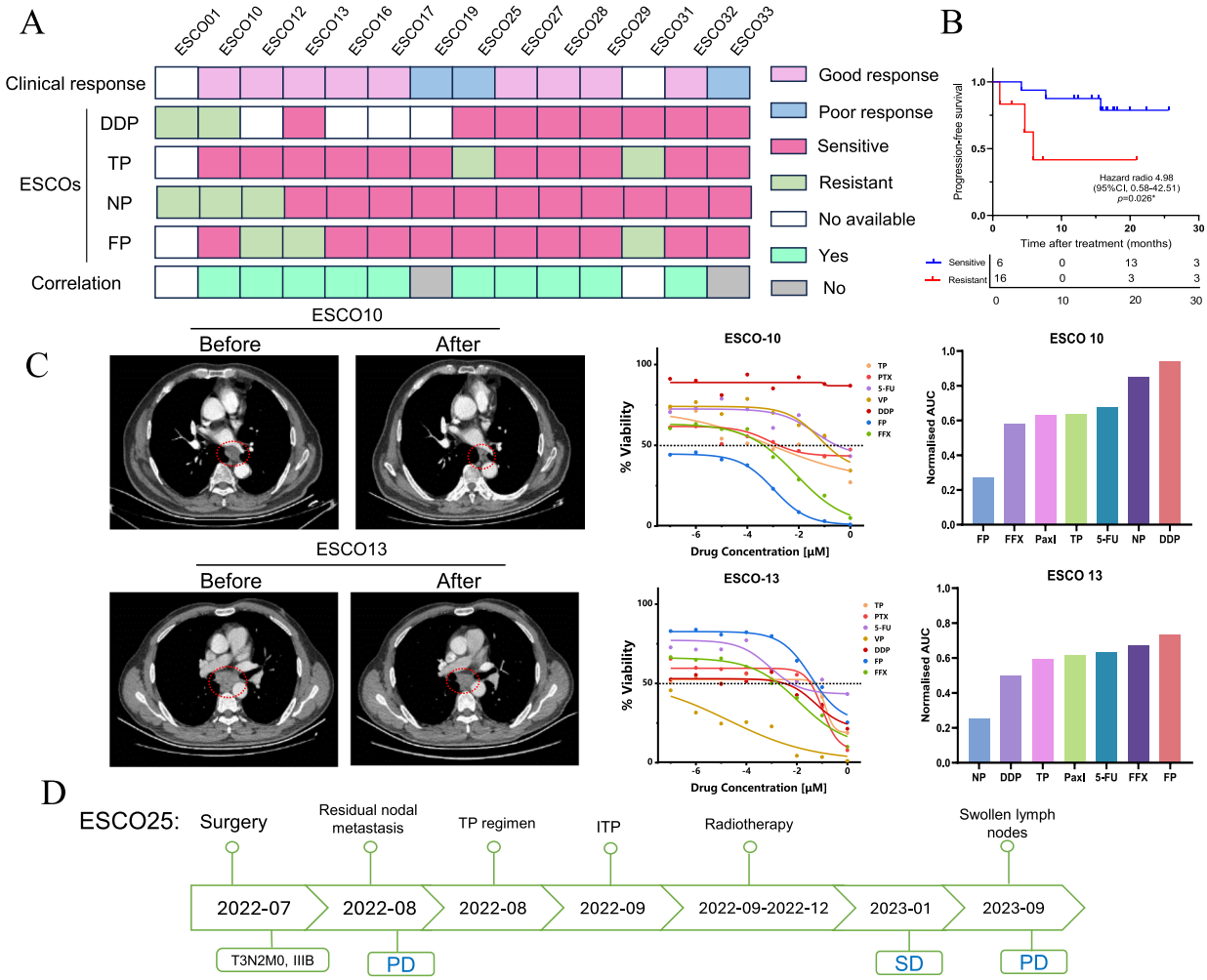

Fig. 5 PDOs Sensitivities Display a Clinical Correlation in ESCC. **A** A heatmap displaying the drug screen results for the 14 evaluable ESCOs and their corresponding patients' clinical responses. **B** Kaplan–Meier curves for patients whose PDOs exhibited drug sensitivity or resistance. **C** CT scans of patients ESCO10 and ESCC13 before and several months after chemotherapy demonstrated tumor size reduction. The corresponding dose–response curves (middle column) and the normalized AUC values (right column) of the ESCOs are presented. **D** Disease progression of ESCO25 was monitored throughout the entire follow-up period. TP: Paclitaxel plus cisplatin; ITP: Immune thrombocytopenia; SD: Stable disease; PD: Progressive disease

The patient subsequently underwent surgery and continued TP treatment postoperatively, maintaining stable disease for over one year through adjuvant chemotherapy. To assess whether PDO profiling reflected the patient's response to chemotherapy, we conducted a drug assay on the ESCOs, revealing distinct sensitivities among various regimens. The AUC of TP ranked highest (AUC = 0.64), indicating that ESCO10 was responsive, aligning with the observed clinical response. A comparable drug response and consistent clinical outcome were also observed in patient ESCO13 (AUC = 0.59). Regarding the resistant case ESCO25 (AUC = 0.78), the patient was diagnosed with ESCC (pT3N2M0, stage IIIB) with perigastric lymph node metastasis, as confirmed by the postoperative pathology report. The patient received adjuvant TP treatment at a local hospital and subsequently underwent adjuvant radiotherapy. Progressive lymph node metastasis was detected 6 months post-surgery, consistent with the resistant response observed in the ESCO (AUC = 0.78). Consequently, the drug response of the PDOs demonstrated both sensitivity and resistance characteristics of their associated tumors Fig. 5D. This preclinical model shows potential value in guiding the selection of appropriate clinical chemotherapy regimens, potentially helping patients avoid ineffective treatments.

Table 2 Clinical response of 14 patients and AUC values of drug screening in corresponding patient-derived organoids

Serial Number	Organoid. ID	Surgery. Date	Time of tissue acquired	Histologic types	Tumor Grade	Tumor Stage	Chemo date	Chemo treatment	Clinical response	Clinical event	RFS (months)	Drug testing (AUC)	Tumor Cellularity (%)	PDOs response	Matched
1	ESCO01	2021/9/22	Chemo-naive	ESCC	2	III	NA	TP	NA	lost to follow-up	1.7	NP = 0.92 5-FU = 1 DDP = 1	72	Resistant	unknow
2	ESCO10	2022/3/24	post-NAT	ESCC	2	III	2021/12/10	TP	PR (2022/1/17)	liver metastasis 2023/3/27	15.7	TP = 0.64 NP = 0.85 FP = 0.27 DDP = 0.94	90	Sensitive	YES
3	ESCO12	2022/4/6	post-NAT	ESCC	2	II	2022/2/11	TP	PR (2022/3/18)	Stable disease 2023/1/31	11.8	TP = 0.69 NP = 0.63 FP = 0.67	74	Sensitive	YES
4	ESCO13	2022/4/12	post-NAT	ESCC	2	III	2021/12/24	TP	PR (2022/2/9)	Lymphatic metastasis 2023/3/31	15.4	TP = 0.59 NP = 0.25 FP = 0.73 CDDP = 0.5	92	Sensitive	YES
5	ESCO16	2022/4/20	post-NAT	ESCC	2	II	2022/2/28	TP	PR (2022/4/7)	Stable disease 2023/12/31	22.4	TP = 0.58 NP = 0.36 FP = 0.36	84	Sensitive	YES
6	ESCO17	2022/5/13	post-NAT	ESCC	1	I	NA	TP	PR (2022/4/18)	Stable disease 2023/12/31	19.9	TP = 0.67 NP = 0.52 FP = 0.58	78	Sensitive	YES
7	ESCO19	2022/5/19	post-NAT	ESCC	2	III	2022/3/16	TP	PR (2022/4/22)	Lymphatic and liver metastasis 2022/7/14	4	TP = 0.33 NP = 0.13 FP = 0.17	95	Sensitive	NO
8	ESCO25	2022/7/8	Chemo-naive	ESCC	1	III	2022/8/9	TP	PD (2023/1/1)	Lymphatic metastasis	5.9	TP = 0.78 NP = 0.58 FP = 0.54 DDP = 0.58	90	Resistant	YES
9	ESCO27	2022/7/15	Chemo-naive	ESCC	3	III	2022/9/5	TP	SD (2023/7/20)	Liver metastasis 2023/9/20	14.4	TP = 0.39 NP = 0.3 FP = 0.41 DDP = 0.55	94.5	Sensitive	YES
10	ESCO28	2022/7/18	Chemo-naive	ESCC	2	III	2022/10/19	S-1	SD 2023/12/31	Stable disease	17.7	TP = 0.60 NP = 0.45 FP = 0.46 DDP = 0.49	85.5	Sensitive	YES
11	ESCO29	2022/7/18	Chemo-naive	ESCC	3	III	2022/9/19	TP	SD 2023/12/31	Stable disease	16.7	TP = 0.57 NP = 0.48 FP = 0.36 DDP = 0.36	94	Sensitive	YES
12	ESCO31	2022/7/20	Chemo-naive	ESCC	2	III	2022/10/13	S-1	NA	lost to follow-up	2.8	TP = 0.75 NP = 0.59 FP = 0.74 CDDP = 0.61	79.5	Resistant	unknow

Table 2 (continued)

Serial Number	Organoid. ID	Surgery. Date	Time of tissue acquired	Histologic types	Tumor Grade	Tumor Stage	Chemo date	Chemo treatment	Clinical response	Clinical event	RFS (months)	Drug testing (AUC)	Tumor Cellularity (%)	PDOs response	Matched
13	ESCO32	2022/7/22	Chemo-naive	ESCC	3	II	2022/9/10	TP	SD 2023/12/31	Stable disease	17.6	TP = 0.65 NP = 0.46 FP = 0.38 DDP = 0.35	85	Sensitive	YES
14	ESCO33	2022/7/27	Chemo-naive	ESCC	3	III	2022/9/16	TP	PD 2022/11/29	Progressive disease 2022/11/29	4.2	TP = 0.43 NP = 0.58 FP = 0.45 DDP = 0.55	85.5	Sensitive	NO

Discussion

EC is an aggressive malignancy with an urgent need for clinical advancements to improve patient outcomes. The ongoing areas of significant interest include early detection and optimizing therapeutic strategies. Emerging research utilizing PDOs aims to validate their sensitivity and specificity as predictive biomarkers for guiding precision medicine, particularly in the context of adjuvant chemotherapy and immunotherapy. This approach has also been applied to other cancers, including liver, breast, colon, pancreatic, and lung cancers [18–21, 38–40]. In 2011, Sato first reported the successful derivation of organoids from human Barrett's epithelium, enabling long-term expansion [41]. Subsequently, the application of PDOs in EC has advanced significantly. Li established a reliable EAC organoid biobank that accurately replicated the phenotypic and molecular characteristics of EAC, facilitating drug screening for novel therapeutic strategies [14]. Concurrently, Kijima et al. developed a robust system for culturing organoids from esophageal and oropharyngeal squamous cell carcinoma patients with high success rates, enabling therapy response evaluation and exploration of underlying mechanisms [22]. However, despite these advancements, the variability in organoid generation success rates across EC subtypes and the complex influence of the tumor microenvironment on drug responses highlights the consistent challenges in standardizing and broadening the use of PDOs for precision medicine. Therefore, further insights into the cellular origin and progression of EC using PDOs hold promise, and studies optimizing drug panel testing for ESCOs and validating these findings through clinical trials are critical for advancing precision medicine and improving therapeutic outcomes.

ESCC accounts for approximately 90% of all EC cases, with particularly high prevalence in Asia and parts of Africa [42]. To advance the feasibility of ESCOs-based approaches, this study presents several novel findings from a multi-institution randomized, retrospective clinical study. First, we established ESCOs with a moderate success rate, demonstrating their ability to recapitulate the morphological heterogeneity and histological characteristics of the matched original tumor tissue across various differentiation statuses and pathological types. Subsequently, we implemented a robust PDOs drug screening platform, utilizing a reliable biobank to assess multi-regimen drug sensitivity, which revealed differential responses of PDOs to conventional chemotherapeutic agents. Furthermore, we corrected real-world clinical outcomes with in vitro drug screening data, indicating high consistency and supporting the integration of translational organoid technologies with personalized therapy. Our approach enables organoid growth within a moderate timeframe, which is clinically relevant, considering that restaging scans are typically performed 2 to 3 months after initiating treatment and serve as criteria for evaluating whether to continue current therapy or switch to alternative treatment [43]. Collectively, these findings support the rapid advancement and significant potential of translating organoid technologies.

A comprehensive analysis of drug sensitivity profiles in 30 ESCOs, evaluating both single and combination regimens, revealed significant variability in organoid responses to various chemotherapeutic treatments and individual drug assays. Notably, a strong correlation was observed between the responses in PDOs and those reported in clinical settings. This correlation aligns with recent retrospective data reported for other cancer types in real-world studies [39, 43]. In contrast to previous studies, this multi-center study introduces a novel classification system using AUCs as the index for assessing PDOs' sensitivities to various treatment regimens, aiming to predict clinical disease control future enrollment of additional cases will enhance the representativeness of this biobank. For chemotherapy-sensitive organoids from a patient expected to respond well to a specific regimen but with an unmatched clinical response, a review of the patient's entire inpatient record revealed an inability to continue chemotherapy cycles due to side effects. This indicates that even when PDO-based drug assays demonstrate high sensitivity to chemotherapy, patients who cannot complete treatment due to adverse effects may experience poor clinical outcomes.This study has several limitations and presents opportunities for future research. While achieving high consistency between organoid drug assays and clinical responses, each sampleoriginated from individual patients during surgery or endoscopic biopsy, including initial tumors and several post-NAT tissues exposed to chemotherapy. However, the absence of paired chemo-naïve and post-chemotherapy samples resulted in missed opportunities to collect materials from the same patient at different disease stages for longitudinal organoid generation [43]. Cancer treatment is a complex, multifaceted, and ongoing process [44]. The variability in treatment effectiveness among patients is intricate and associated with numerous factors, including post-operative outcomes, combination therapies, chemotherapy side effects, overall health conditions, and tumor characteristics [45]. Although the chemosensitivity of organoids may partially reflect the tumor's response at a specific time, it has limitations in capturing tumor evolution and changes in overall drug treatment response. Another challenge is the limited source of tissue, all samples were acquired from patients in suitable condition for surgical resection, which

excludes tumor tissues from advanced stages and metastatic sites, limiting the comprehensive of the biobank. To address this, incorporating tissue from advanced and metastatic tumors to generate a more representative biobank, along with more extensive genomic validation in future studies, would be valuable, particularly for testing targeted drugs and determining patient eligibility for precision clinical trials.It is noteworthy that the success rate of ESCC organoid generation was lower and requires enhancement compared to other cancer types, such as colorectal cancer, breast cancer, and other adenocarcinoma cancers [12, 15, 38]. This disparity and associated challenges potentially stem from the inherent heterogeneity of squamous cell carcinoma and its dependence on specific stromal interactions and extracellular matrix components, which are challenging to replicate in standard organoid cultures [46]. Adenocarcinoma, originating from glandular structures in epithelial tissue, typically exhibits more predictable growth patterns, facilitating well-established organoid culture protocols [41]. Sachdeva et al. reported developing reliable protocols to establish PDOs from EAC with an 80% success rate, compared to their 60% success rate in ESCC organoids generation [46]. While we did not initially control the source of samples, due to the prevalence of EC in our region, all samples included in this study were diagnosed as ESCC through professional histological analysis. Future studies should incorporate various histological subtypes, as ongoing technological advancements and refined cultural conditions are expected to gradually mitigate the challenges associated with organoid generation. In addition to tumor organoids, the tumor microenvironment, composed of stromal cells and inflammatory cells, plays a crucial role in influencing tumor behavior and drug-resistant mechanisms47. Co-culture models that generate patient-derived organoids in combination with non-cancerous cells represent promising approaches to better facilitate cellular repopulation and tissue regeneration, capturing the heterogeneous features of the original tumor environment in vitro.

Conclusion

In summary, this study demonstrates that PDO-based drug assays provide significant insights into the efficacy of standard treatments for ESCC patients. The successful generation of PDOs from a heterogeneous cohort of ESCC patients within a clinically relevant timeframe resulted in findings that strongly correlate with individual clinical outcomes and drug sensitivity profiles, highlighting the potential of these models for addressing clinical translational questions and providing thoughtful insights into personalized treatment strategies

Abbreviations

EAC	Esophageal adenocarcinoma
EC	Esophageal carcinoma
ESCC	Esophageal squamous cell carcinoma
ESCOs	Esophageal squamous cell carcinoma organoids
PDOs	Patient-derived organoids

Supplementary Information

The online version contains supplementary material available at https://doi.org/10.1186/s12967-024-05967-1.

Supplementary material 1

Acknowledgments

We extend our gratitude to all patients and their families who participated in this study and generously contributed their samples. Furthermore, we acknowledge the invaluable support of our clinical and research team members for their assistance with tissue collection and processing.

Author contributions

Suya Shen (Conceptualization, methodology, writing original draft, data curation). Jingjing Li (Conceptualization: Lead; Funding acquisition; Investigation; Supervision; Supporting). Zheng Hongping, Bing Liu (Original draft writing; Formal analysis). Wei Ren, Yudong Qiu (Supervision; validation). Wenyan Guan (Histology analysis: Supporting; Investigation). Jian He, Zhiwen Li, Weifeng Tang, Pengju Zhang (Data analysis; Methodology). Yuqing Han, Yingzhe Hu (Data collection, writing—review and editing: Equal). Ziyao Liu, Yiqiang Chen, Siyuan Liu (Sample acquisition, data collection).

Funding

This research was funded by the National Nature Science Foundation of China (No. 82372988), the Health Technology Development Project of Nanjing City (No. YKK21077), and the Clinical Trials funding from the Affiliated Drum Tower Hospital, Medical School of Nanjing University (No. 2022-LCYJ-PY-03). Suya Shen received support from the China Scholarship Council (No. 202306190025).

Data availability

All data supporting the findings of this study are included in the paper and its Supplementary Information.

Declarations

Competing interests

Suya Shen, Bin Liu, and Wenyan Guan contributed equally to this work. The authors declare that no members of the research team were involved in any commercial or financial relationships that could be construed as a potential conflict of interest.

Author details

[1]Department of Pancreatic and Metabolic Surgery, Nanjing Drum Tower Hospital, Affiliated Hospital of Medical School, Nanjing University, Nanjing 210008, China. [2]Key Laboratory of Carcinogenesis and Translational Research (Ministry of Education/Beijing), Department of Thoracic Surgery II, Peking University Cancer Hospital & Institute, Beijing 100142, China. [3]Department of Pathology, Nanjing Drum Tower Hospital, The Affiliated Hospital of Nanjing University Medical School, Nanjing 210008, Jiangsu, China. [4]Department of Precision Medicine, Nanjing Drum Tower Hospital, The Affiliated Hospital of Nanjing

University Medical School, Nanjing 210008, Jiangsu, China. [5]Department of Pancreatic and Metabolic Surgery, Nanjing Drum Tower Hospital Clinical College of Nanjing University of Chinese Medicine, Nanjing 210008, Jiangsu, China. [6]Department of Nuclear Medicine, Nanjing Drum Tower Hospital, Affiliated Hospital of Nanjing University Medical School, Nanjing 210008, Jiangsu, China. [7]Department of Esophageal Surgery, Nanjing Drum Tower Hospital, Affiliated Hospital of Nanjing University Medical School, NanjingJiangsu 210008, China. [8]Zhejiang Honray Medical Technology Co., LTD, Taizhou 318001, Zhejiang, China. [9]The Comprehensive Cancer Center of Drum Tower Hospital, Medical School of Nanjing University & Clinical Cancer Institute of Nanjing University, Nanjing 210008, Jiangsu, China. [10]Shanghai Institute for Biomedical and Pharmaceutical Technologies, Shanghai 200032, China.

Received: 29 October 2024 Accepted: 11 December 2024
Published online: 31 December 2024

References

1. Rustgi AK, El-Serag HB. Esophageal carcinoma. N Engl J Med. 2014;371:2499–509.
2. Ishihara R, Arima M, Iizuka T, et al. Endoscopic submucosal dissection/endoscopic mucosal resection guidelines for esophageal cancer. Dig Endosc. 2020;32:452–93.
3. Kitagawa Y, Ishihara R, Ishikawa H, et al. Esophageal cancer practice guidelines 2022 edited by the Japan Esophageal Society: part 2. Esophagus. 2023;20:373–89.
4. Ishihara R, Tani Y, Okubo Y, et al. Endoscopic landmarks corresponding to anatomical landmarks for esophageal subsite classification. DEN Open. 2024;4: e273.
5. Prigerson HG, Bao Y, Shah MA, et al. Chemotherapy use, performance status, and quality of life at the end of life. JAMA Oncol. 2015;1:778–84.
6. Ooft SN, Weeber F, Dijkstra KK, et al. Patient-derived organoids can predict response to chemotherapy in metastatic colorectal cancer patients. Sci Transl Med. 2019;11:513.
7. Villaflor VM, Allaix ME, Minsky B, et al. Multidisciplinary approach for patients with esophageal cancer. World J Gastroenterol. 2012;18:6737–46.
8. Sheikh M, Roshandel G, McCormack V, et al. Current status and future prospects for esophageal cancer. Cancers. 2023;15:765.
9. Rogers JE, Sewastjanow-Silva M, Waters RE, et al. Esophageal cancer: emerging therapeutics. Expert Opin Ther Targets. 2022;26:107–17.
10. Vanden Heuvel JP, Maddox E, Maalouf SW, et al. Replication study: systematic identification of genomic markers of drug sensitivity in cancer cells. Elife. 2018. https://doi.org/10.7554/eLife.29747.
11. Barretina J, Caponigro G, Stransky N, et al. Addendum: The Cancer Cell Line Encyclopedia enables predictive modelling of anticancer drug sensitivity. Nature. 2019;565:E5–6.
12. Tiriac H, Belleau P, Engle DD, et al. Organoid profiling identifies common responders to chemotherapy in pancreatic cancer. Cancer Discov. 2018;8:1112–29.
13. Yang R, Yu Y. Patient-derived organoids in translational oncology and drug screening. Cancer Lett. 2023;562: 216180.
14. Li X, Francies HE, Secrier M, et al. Organoid cultures recapitulate esophageal adenocarcinoma heterogeneity providing a model for clonality studies and precision therapeutics. Nat Commun. 2018;9:2983.
15. Chen P, Zhang X, Ding R, et al. Patient-derived organoids can guide personalized-therapies for patients with advanced breast cancer. Adv Sci. 2021;8: e2101176.
16. Kucherlapati R. Genetically modified mouse models for biomarker discovery and preclinical drug testing. Clin Cancer Res. 2012;18:625–30.
17. Yoshida GJ. Applications of patient-derived tumor xenograft models and tumor organoids. J Hematol Oncol. 2020;13:4.
18. Xie C, Gu A, Khan M, et al. Opportunities and challenges of hepatocellular carcinoma organoids for targeted drugs sensitivity screening. Front Oncol. 2022;12:1105454.
19. Driehuis E, van Hoeck A, Moore K, et al. Pancreatic cancer organoids recapitulate disease and allow personalized drug screening. Proc Natl Acad Sci USA. 2019;116:26580–90.
20. Chen P, Zhang X, Ding RB, et al. Patient-derived organoids can guide personalized-therapies for patients with advanced breast cancer. Adv Sci. 2021;8:22.
21. Su C, Olsen KA, Bond CE, et al. The efficacy of using patient-derived organoids to predict treatment response in colorectal cancer. Cancers. 2023;15:805.
22. Kijima T, Nakagawa H, Shimonosono M, et al. Three-dimensional organoids reveal therapy resistance of esophageal and oropharyngeal squamous cell carcinoma cells. Cell Mol Gastroenterol Hepatol. 2019;7:73–91.
23. Whelan KA, Muir AB, Nakagawa H. Esophageal 3D culture systems as modeling tools in esophageal epithelial pathobiology and personalized medicine. Cell Mol Gastroenterol Hepatol. 2018;5:461–78.
24. Lin L, Lin DC. Biological significance of tumor heterogeneity in esophageal squamous cell carcinoma. Cancers. 2019;11:1156.
25. Eisenhauer EA, Therasse P, Bogaerts J, et al. New response evaluation criteria in solid tumours: revised RECIST guideline (version 1.1). Eur J Cancer. 2009;45:228–47.
26. Hirokawa Y, Clarke J, Palmieri M, et al. Low-viscosity matrix suspension culture enables scalable analysis of patient-derived organoids and tumoroids from the large intestine. Commun Biol. 2021;4:1067.
27. Then EO, Lopez M, Saleem S, et al. Esophageal cancer: an updated surveillance epidemiology and end results database analysis. World J Oncol. 2020;11:55–64.
28. Sakuramoto S, Sasako M, Yamaguchi T, et al. Adjuvant chemotherapy for gastric cancer with S-1, an oral fluoropyrimidine. N Engl J Med. 2007;357:1810–20.
29. Vlachogiannis G, Hedayat S, Vatsiou A, et al. Patient-derived organoids model treatment response of metastatic gastrointestinal cancers. Science. 2018;359:920–6.
30. Kaufmann O, Fietze E, Mengs J, et al. Value of p63 and cytokeratin 5/6 as immunohistochemical markers for the differential diagnosis of poorly differentiated and undifferentiated carcinomas. Am J Clin Pathol. 2001;116:823–30.
31. Zhong L, Li H, Chang W, et al. TP53 Mutations in Esophageal Squamous Cell Carcinoma. Front Biosci. 2023;28:219.
32. Sankalecha TH, Gupta SJ, Gaikwad NR, et al. Yield of p53 expression in esophageal squamous cell cancer and its relationship with survival. Saudi J Gastroenterol. 2017;23:281–6.
33. Luo Y, Chen C. The roles and regulation of the KLF5 transcription factor in cancers. Cancer Sci. 2021;112:2097–117.
34. Yang Y, Goldstein BG, Chao HH, et al. KLF4 and KLF5 regulate proliferation, apoptosis and invasion in esophageal cancer cells. Cancer Biol Ther. 2005;4:1216–21.
35. Diao FY. Organoid models combined with genome engineering and epigenome studies to define SOX2 function evolution in esophageal squamous cell carcinoma. Thorac Cancer. 2021;12:2635–6.
36. Zhang J, Wang Z, Zhao H, et al. The roles of the SOX2 protein in the development of esophagus and esophageal squamous cell carcinoma, and pharmacological target for therapy. Biomed Pharmacother. 2023;163: 114764.
37. Jiang YY, Jiang Y, Li CQ, et al. TP63, SOX2, and KLF5 establish a core regulatory circuitry that controls epigenetic and transcription patterns in esophageal squamous cell carcinoma cell lines. Gastroenterology. 2020;159(1311–1327): e19.
38. Tan T, Mouradov D, Lee M, et al. Unified framework for patient-derived, tumor-organoid-based predictive testing of standard-of-care therapies in metastatic colorectal cancer. Cell Rep Med. 2023;4: 101335.
39. Wang HM, Zhang CY, Peng KC, et al. Using patient-derived organoids to predict locally advanced or metastatic lung cancer tumor response: a real-world study. Cell Rep Med. 2023;4: 100911.
40. Takahashi N, Hoshi H, Higa A, et al. An In vitro system for evaluating molecular targeted drugs using lung patient-derived tumor organoids. Cells. 2019;8:481.
41. Sato T, Stange DE, Ferrante M, et al. Long-term expansion of epithelial organoids from human colon, adenoma, adenocarcinoma, and Barrett's epithelium. Gastroenterology. 2011;141:1762–72.
42. Abnet CC, Arnold M, Wei WQ. Epidemiology of esophageal squamous cell carcinoma. Gastroenterology. 2018;154:360–73.

43. Demyan L, Habowski AN, Plenker D, et al. Pancreatic cancer patient-derived organoids can predict response to neoadjuvant chemotherapy. Ann Surg. 2022;276:450–62.
44. Liu B, Zhou H, Tan L, et al. Exploring treatment options in cancer: tumor treatment strategies. Signal Transduct Target Ther. 2024;9:175.
45. Miller KD, Nogueira L, Devasia T, et al. Cancer treatment and survivorship statistics, 2022. CA Cancer J Clin. 2022;72:409–36.
46. Sachdeva UM, Shimonosono M, Flashner S, et al. Understanding the cellular origin and progression of esophageal cancer using esophageal organoids. Cancer Lett. 2021;509:39–52.
47. Zheng S, Liu B, Guan X. The role of tumor microenvironment in invasion and metastasis of esophageal squamous cell carcinoma. Front Oncol. 2022;12:911285.

Publisher's Note